

## Deposition and Characterization of Sisal Fiber Composite Prepare By Iron Oxide Synthesis.

Asif Jehan\*, Dr. Shirish Joshi\*\* and Dr. M.N. Bapat\*\*\*

\*, \*\* Motilal vigyan mahavidhalya Bhopal (M.P.) India

\*\*\*Regional institute of education Bhopal (M.P.) India

### Abstract

Iron oxide synthesized through sintering route. The present research work deals with ferrite composite prepared using chemical reactions. Ferric nitrates and ammonium chloride doped with sisal fiber has been prepared. The comparative studies of ferric oxide were examined through few characterizations. The structural behavior of iron oxide was studied in XRD, FT/IR, TEM and SEM. This behavior showed ferrite nature of the sample.

**Key words:** -  $\text{Fe}_2\text{O}_3$ , sintering method, TEM, SEM, XRD AND FT/IR

### I. Introduction

Iron oxides are chemical compounds composed of iron and oxygen. All together, there are sixteen known iron oxides and oxyhydroxides. [1] Iron (III) oxide or ferric oxide is the inorganic compound with the formula  $\text{Fe}_2\text{O}_3$ . It is one of the three main oxides of iron, the other two being iron (II) oxide (FeO), which is rare, and iron (II, III) oxide ( $\text{Fe}_3\text{O}_4$ ), which also occurs naturally as the mineral magnetite. As the mineral known as hematite,  $\text{Fe}_2\text{O}_3$  is the main source of the iron for the steel industry.  $\text{Fe}_2\text{O}_3$  is ferromagnetic, dark red, and readily attacked by acids. Rust is often called iron(III) oxide, and to some extent this label is useful, because rust shares several properties and has a similar composition.

The steelmaking by-products such as dust and mill scale, very rich in iron ( $\approx 72\%$  Fe), are currently produced in large quantities and represent a potential of almost 5 million tons in the world [2]. Generally, these by-products are recycled by the metallurgical processes such as the blast furnace or the direct reduction reactors that uses coal as reducing agent to produce pre-reduced pellets intended for the remelt in electric steel plant. Besides the steelmaking, recycling part of these by-products is already supported by the powder metallurgy where the economic recovery is more favorable. During the last twenty years, powder metallurgy has presented a continued expansion in all its aspects and in all of its applications to the industry. Powder metallurgy comprises a set of processes of forming having for common denominator a raw material in a powder form. The reduced iron powder is the most widely used material in powder metallurgy industry. The direct reduction process has commonly been used by many companies (such as Hoeganas in Sweden, Kawasaki in Japan and Pyron in US) to obtain metallic iron powder by the reaction of iron oxide

(magnetite, hematite ore or mill scale) and reducing gases ( $\text{CO}/\text{H}_2$ ) under high temperatures ( $> 1000^\circ\text{C}$ ) [3]. The reduction of iron oxides and various ores containing iron oxides have been studied in the past [4-9]. Their researches are conducted using as reducing agents solid carbon and reducing gas ( $\text{CO}$  and/or  $\text{H}_2$ ).

During the recent years, there has been a great deal of interest in bio composites containing magnetite ( $\text{Fe}_3\text{O}_4$ ) nano particles dispersed in polymeric, glassy or ceramic matrices. Iron oxide nano particles present a great scientific interest in technological applications such as high – density magnetic recording media, biosensors, ferro fluids, magnetic resonance imaging, biomedicine. Biomedical applications require iron-oxide nano particles with size smaller than 20 nm and a narrow size distribution. The properties of these materials depend strongly on the particle size, the particle-matrix interactions and the disposal of the nano particles in the matrix [10-16].

According to GERMAN SALAZAR-ALVAREZ thesis this deals with the synthesis, characterization, and some applications of ferromagnetic iron oxide nano particles. The iron oxide systems presented in this work are  $\text{Fe}_3\text{O}_4$ ,  $\text{Fe}_2\text{O}_3$ ,  $\text{Ni}_x\text{Fe}_{3-x}\text{O}_4$ , and  $\text{Co}_x\text{Fe}_{3-x}\text{O}_4$ . Iron oxide nano particles were prepared using chemical synthesis methods. Nano particles with a narrow size distribution were synthesized using zone confinement methods such as nano emulsions and a novel flow injection synthesis. The flow injection method consisted of the precipitation of iron oxide nano particles in a continuous or segmented flow in a capillary reactor under laminar flow. [17]

### II. Process

The method of making alumina comprise of following steps...

Firstly provide a growing substrate and growing device, comprising a heating apparatus with reacting chamber. Secondly placing growing substrate and a quantity of reacting materials into the reaction chamber. Lastly, heating the reaction chamber to a temp 1000o C the steps are following:-

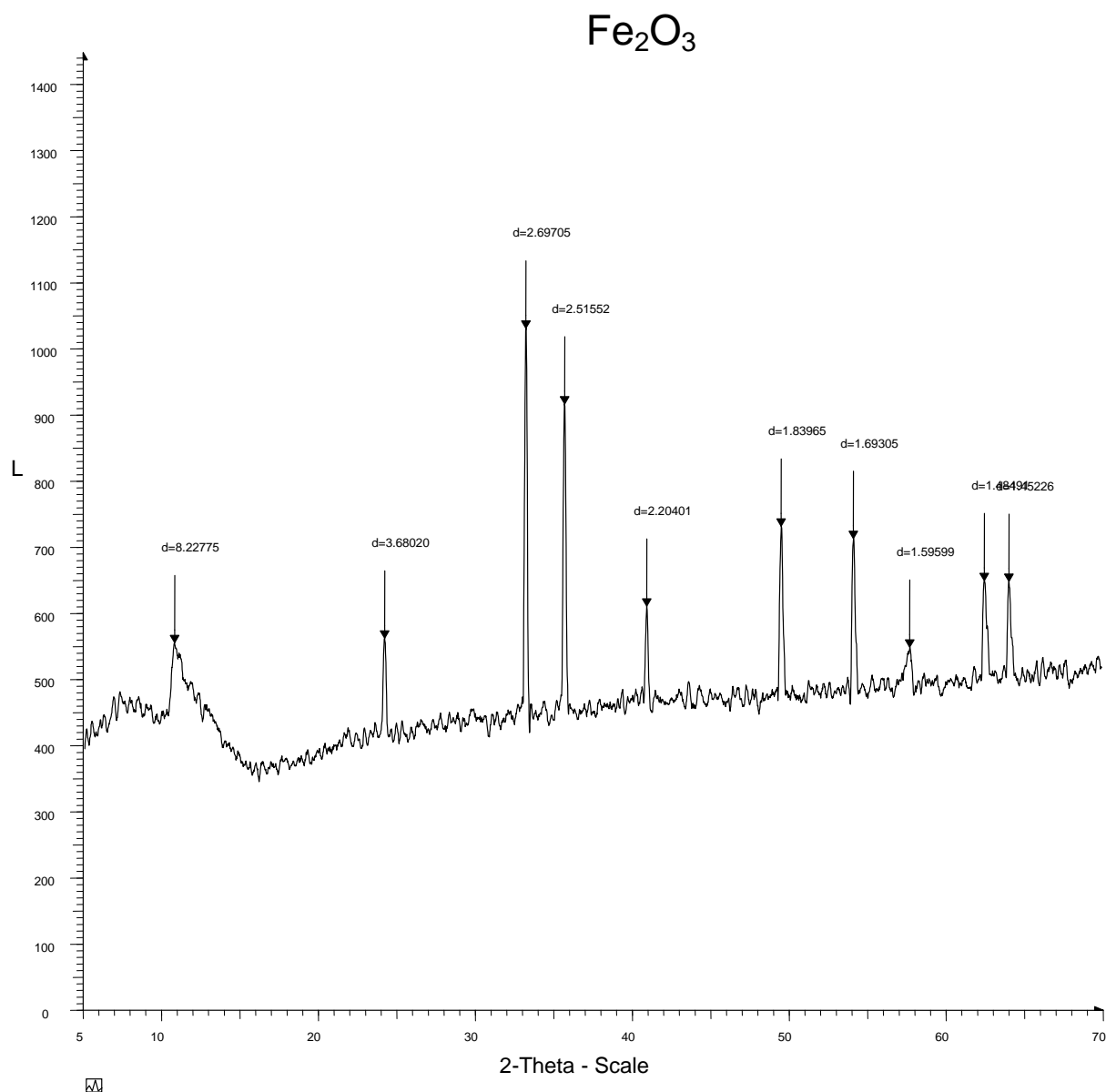
- Take a quantity of ferric nitrate and ammonium chloride and dissolve it into water.
- Now putted the sisal fiber in this solution and left it for 1 hour.
- After 1 hour we added the drops (10 d) of ammonia solution into this solution.
- Putting this solution to a temperature 1000° C to obtain alumina.
- Taken out the crucible containing material and placed it on asbestos sheet till it cools down to room temperature.

### III. Result and discussion

#### XRD

The amorphous state of the sisal fiber composite was verified by XRD. The x-ray diffraction patterns of Fe<sub>2</sub>O<sub>3</sub> doped with sisal fiber shown in fig 1. The

main peaks for Fe<sub>2</sub>O<sub>3</sub> are observed at 2θ=10.744 (d=8.22775 Å), 2θ=24.164 (d=3.68020 Å), 2θ=33.190 (d=2.69705 Å), 2θ=35.663 (d=2.51552 Å), 2θ=40.913 (d=2.20401 Å), 2θ=49.508 (d=1.83965 Å), 2θ=54.127 (d=1.69305 Å), 2θ=57.717 (d=1.59599 Å), 2θ=62.497 (d=1.48491 Å), 2θ=64.067 (d=1.45226 Å) corresponding to (555), (562), (1032), (917), (611), (732), (713), (548), (649) and (648) reflections. The peaks present in Fe<sub>2</sub>O<sub>3</sub> were also observed in the composition of sisal fiber with Fe<sub>2</sub>O<sub>3</sub> which indicates the presence of ferrite particle. The entire pattern indicates about the small dimensions of the iron oxide particles. The changes in peaks occur due to the presence of composition of sisal fiber [18]. These radical cations through the coupling reaction lead to the ion of stable electrically conducting natural fiber. Reaction with the natural fiber generated by an internal redox reaction, which casus the reorganization of electronic structure to give the +ve and -ve nature of a radical is linked to its difference in reactivity towards lignin and cellulose/hemicelluloses [19].



Natural sisal fiber consists of proton H<sup>+</sup> molecule in its composition and deprotonation process is also occurred in natural fiber. Deprotonation is the removal of a proton (H<sup>+</sup>) from a molecule. Deprotonation of the radical cation is a

major pathway and the proton removal decreases positive charge in the molecule and an increases negative charge. Deprotonation usually occurs from the donation of electrons or acceptance of the proton using a base, which forms its conjugate acid. [20]

Name	Symbol	Classification	A	B
Cellulose	C <sub>6</sub> H <sub>10</sub> O <sub>5</sub>	C-H Deprotonation	C	H
Hemicelluloses	C <sub>5</sub> H <sub>10</sub> O <sub>5</sub>	C-H Deprotonation	C	H
Lignin	C <sub>13</sub> H <sub>34</sub> O <sub>11</sub>	C-H Deprotonation	C	H

### TEM

Fig 2 (a) (b) and (c) shows the non linear and non uniform dispersed iron oxide particles of 141.24nm and the agglomerated fiber containing 30.31-30.90nm size particles of iron oxide. The samples appear highly strained as seen in fig 2 (a) (b) and (c).

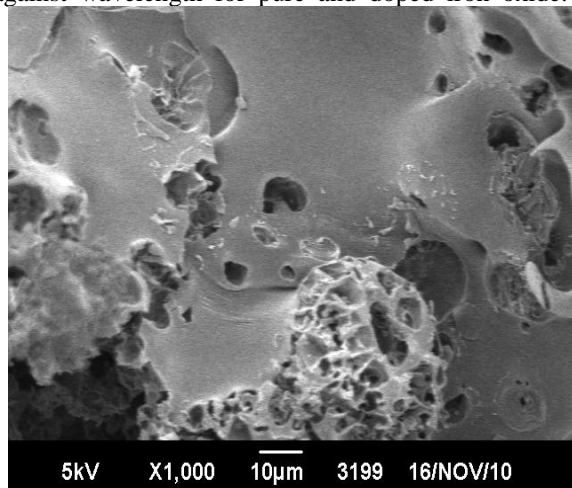


Fig 2 (a), (b) and (c)

The presence of dislocation loops is clearly seen. It is possible that the strain present in the sintered samples has a direct effect on the dielectric loss.

### SEM

Figure 3 (a) and (b) shows the morphology of  $Fe_2O_3$ . The micrograph depicts the crystalline nature. The variation in specular optical transmittance against wavelength for pure and doped iron oxide.



This shows the typical micrograph of the clustering of well established randomly oriented nano rods which has compact, homogenous and well adherent growth onto the substrate. Fig (a) and (b) shows the morphology of material and fiber respectively. Fig 3(a) has porosity, non uniform and inside hollow texture. Its upper surface is in crystalline, non linear, soft and spongy form. In fig 3(b) fiber shows a crystalline, linear and smoky effect.

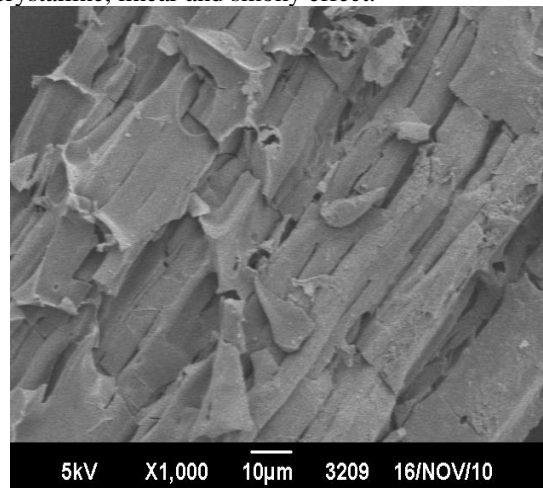


Fig 3 (a) and (b)

### FTIR

It is clear from fig 4 that broad absorption bands appear at 6188.9515, 2721.0889 and 2592.8639  $cm^{-1}$  respectively, which are attributed to the stretching vibration of hydroxyl groups. The peaks at 3437.2197, 3409.4926 and 3125.4871  $cm^{-1}$  correspond to the vibration of carboxylic acid groups. The IR transmission spectra of sisal fiber composite

were recorded in the range 500-4000  $cm^{-1}$ . The prepared sample was free from visible inhomogeneities like cracks or bubbles. Decrease with a shifting of meta-center towards slightly higher wave number. For further increase of  $Fe_2O_3$  the intensity of this band is continued to decrease where the first group of bands is also observed to decrease. [21]

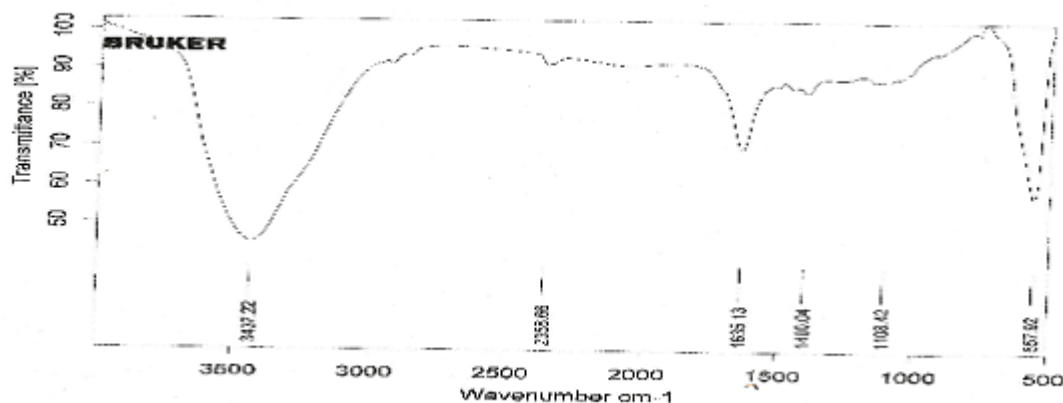


Fig 4

#### IV. Conclusion

The ferric oxide synthesized by the sintering method has shown deprotonation behavior. H releases from deprotonation process which is responsible for conduction and it is shown in SEM &TEM.

#### Reference

- [1.] Cornell, RM; Schwertmann, U (2003). *The iron oxides: structure, properties, reactions, occurrences and uses*. Wiley VCH. ISBN 3-527-30274-3.
- [2.] Bienvenu, Y., Rodrigues, S. *Manufacture of Metal Powders from Pulverulent Waste, ENSMP, Centre des matériaux, CNRS UMR 7633, France* (2007).
- [3.] Bouvard, D. *Métallurgie des poudres*, Paris, Hermès Science Publications, (2002).
- [4.] Pyron Expands Across the Powder Range. MPR, (1995).
- [5.] Pineau, A., Kanariand, N., Gaballah, I. Kinetics of Reduction of Iron Oxides by H<sub>2</sub>, Part I: Low Temperature Reduction of Hematite, *Thermochimica Acta*, 447 (2006) 89.
- [6.] Pineau, A., Kanariand, N., Gaballah, I. Kinetics of Reduction of Iron Oxides by H<sub>2</sub>, Part II : Low Temperature Reduction of Magnetite, *Thermochimica Acta*, 456 (2007) 75. 7. Kohl, H.K., Marincek, B. Kinetics of the Reduction of Iron Oxides with Graphite, *Archiv Fur das Eisen*, 36 (1965) 851.
- [7.] El-Geasy, A.A., Nasr, M.I. Influence of Original Structure on the Kinetics and Mechanisms of Carbon Monoxide Reduction of Hematite Compacts. *ISIJ International*, 30 (1990) 417.
- [8.] Martín, M.I., López, F.A. Obtainment of Sponge Iron by Reduction of a Steel Making By-Product, 1st Spanish
- [9.] National Conference on Advances in Materials Recycling and Eco-energy, Madrid, (2009) 12.
- [10.] R. M. Cornell, U. Schwertmann, *The Iron Oxides*; Wiley-VCH: Weinheim, Germany, (2003).
- [11.] J. M. Perez, F. J. Simeone, Y. Saechi, L. Josephson, R. J. Weissleder, *Am. Chem.Soc.* **125**, 10192 (2003).
- [12.] A. I. Anton, J. Magn. *Magn. Mater.* **85**, 137 (1990).
- [13.] P. Oswald, O. Clement, C. Chambon, E. Claeys, E. Fuja, G. Magn. *Reson. Imaging* **15**, 1025 (1997).
- [14.] L. Fu, V. P. Dravid, D. L. Jhonson, *Appl. Surf. Sci.* **181**, 173 (2001).
- [15.] D. L. Leslie-Pelecky, *Chem. Mater.* **8**, 1770 (1996).
- [16.] E. M. Moreno, M. Zayat, M. P. Morales, C. J. Serna, A. Roig, D. Levy, *Langmuir* **18**, 4972 (2002).
- [17.] <http://www.met.kth.se/drweb/abstracts/german-salazaralvarez2.pdf>
- [18.] s.k. dhawan kuldeep singh, anil, a.k. bakhshi polymeric & soft materials section. National physical laboratory. New delhi-110021. India
- [19.] ek et al. 1989
- [20.] Schmittle, M.; Burghart, A. *Angew. Chem. int. Ed. EEngl.* 1997, 36, 2550.
- [21.] S yusub, Gsahaya baskaranet al *Indian journal of pure & applied physics* Vol. 49 May 2011. Pp 315-322.